J Mater Sci: Mater Electron (2014) 25:3639–3644
DOI 10.1007/s10854-014-2068-y

Advanced research into the growth mechanism and optical properties of wurtzite ZnSe quantum dots

Donglai Han · Bo Feng · Jian Cao · Ming Gao · Shuo Yang · Jinghai Yang

Received: 14 April 2014 / Accepted: 1 June 2014 / Published online: 6 June 2014

Abstract Zinc selenide (ZnSe) quantum dots (QDs) with the hexagonal wurtzite structure were successfully prepared using a safe, controllable ethylenediamine-mediated solvothermal method in the absence of surfactants. This new synthesis process of the wurtzite ZnSe QDs was described and the growth mechanism of QDs was proposed. The room-temperature photoluminescence (PL) spectrum of the wurtzite ZnSe QDs (about 4 nm) showed a strong near-band-edge emission peak at 422 nm. The near-band-edge emission peak was blue-shifted compared to that of the bulk ZnSe due to the quantum confinement effects; the peak also displayed a progressive red-shift with increasing the excitation power and an associated reduction in peak energy of up to 300 meV. Band gap renormalization in the electron–hole plasma regime might be used to explain this phenomenon. No previous published research regarding the observed excitation-power-dependent PL properties of the wurtzite ZnSe QDs had been found. Our experimental results contributed valuable insights into the optical properties of the wurtzite ZnSe QDs; with potential applications in optoelectronics and other areas where advanced uniformly-structured nanocrystalline semiconductor materials were finding increased use.

D. Han · S. Yang · J. Yang
Changchun Institute of Optics, Fine Mechanics and Physics, Chinese Academy of Sciences, Changchun, 130033, People's Republic of China

D. Han · S. Yang · J. Yang
University of Chinese Academy of Sciences, Beijing 100049, People's Republic of China

B. Feng (✉) · J. Cao · M. Gao · J. Yang (✉)
Key Laboratory of Functional Materials Physics and Chemistry of the Ministry of Education, Jilin Normal University, Haifeng Street No. 1301, Siping 136000, People's Republic of China
e-mail: fengbosiping@126.com

J. Yang
e-mail: jhyang1@jlnu.edu.cn

1 Introduction

Nanometer-scaled semiconductor crystallites, commonly known as quantum dots (QDs), have been gaining popularity due to their unique optical properties and potentially wide applications in optoelectronics, biomedical labeling, photocatalysis, and enhanced photovoltaic solar cells [1–5]. QDs are spherical nanoparticles that have diameters less than the bulk excitonic Bohr radius. Their energy bands have discrete levels and their electrons and holes are independently confined [6–8]. QDs are very promising as photoluminescence (PL) emitters due to their high stability, PL quantum yield, and the tunability of emission and absorption properties with nanoparticle sizes [9–11]. The tunability plays a significant role in the optical properties of QDs by broadening the spectral range of certain types of nanocrystal semiconductors [11, 12]. Zinc selenide (ZnSe) is an II–VI semiconductor with a bulk band gap of 2.67 eV, which makes it highly suited for use in optoelectronic devices and photovoltaic solar cells applications [13, 14]. ZnSe has a very large excitonic binding energy (21 meV) compared with GaAs (4.2 meV), and is an excellent choice in efficient room-temperature excitonic devices that offer improved temperature characteristics [15, 16]. Unlike cadmium-based QDs that exhibit high toxicity and a green to infrared fluorescence spectral range [17–21], ZnSe is non-toxic and environment-friendly, and most importantly, ZnSe

QDs are wide band gap nanomaterials with excellent UV-blue emission characteristics, making them well suited to a widening range of commercial and scientific nanotechnology applications [22–24]. Uniformly-structured ZnSe QDs can be synthesized using a variety of methods, however, most attempts to date have been proven unsafe, difficult to implement, and not commercially viable. For example, the use of diethyl zinc as a Zn precursor leads to highly toxic, expensive, potentially flammable processes requiring careful handling and stringent oxygen-free anhydrous conditions [25]. The control of particle size and uniformity during the QDs synthesis has also presented significant challenges, and most published reports relate to the cubic modification of ZnSe (i.e., zinc blende structure). Very little has been published on ZnSe QDs with the hexagonal wurtzite structure, and the wurtzite structure offers key benefits that include strong quantum-size effects and improved uniformity, which are prerequisites for efficient nanosheet fabrication.

ZnSe is attracting increased attention due to recent advancements in crystal quality and related growth techniques [26, 27]. An important goal in synthesizing ZnSe-based QDs is to achieve room-temperature operation of blue and green laser diodes with long lifetimes. In order to slow down the rapid degradation process of ZnSe-based materials, much effort has been made to improve the crystalline quality of the ZnSe-based materials. We believe that the real degradation mechanisms are as yet unclear, and further research is warranted, to correctly understand the design, operation and performance characteristics of the ZnSe-based devices [28–30]. Some researchers consider that the ZnSe-based devices may fail due to the presence of high density optical fields within the device and their effects on the fragile chemical bonds between the Zn and Se atoms [31]. Therefore, a thorough investigation of the excitation-power-dependent PL behaviors of ZnSe materials is also considered important, since no published research has been found on this aspect of the PL behaviors of the ZnSe QDs with the hexagonal wurtzite structure.

In this paper, we synthesize the wurtzite ZnSe QDs successfully using the solvent method, and the experimental measurements are conducted to characterize the room-temperature and the excitation-power-dependent PL properties of the wurtzite ZnSe QDs. Our method of aqueous synthesis of ZnSe QDs offers certain advantages, including a moderate reaction temperature, the use of low-toxicity chemicals and water-soluble products. The growth mechanism of the ZnSe QDs is discussed in detail. A simple method of adjusting an external light beam to manipulate the PL characteristics of the QDs is also uncovered that may provide valuable insights for further research on adjustable optoelectronic devices, and the study of other nanoscaled semiconductors.

2 Experimental

2.1 Preparation of ZnSe QDs

All chemicals were of analytical grade and used as received without further purification. The synthesis of the ZnSe precursor was carried out using the following procedures: $Zn(NO_3)_2{\cdot}6H_2O$ (0.5 mmol) was dissolved in 30 ml water and selenium powder (99.95 %) (0.5 mmol) in 30 ml of ethylenediamine (EN). After stirring for 1 h, water and EN were added into one beaker. Then after stirring for a further hour, the mixed solution was transferred into one 80-ml Teflon-lined autoclave. The autoclave was sealed and heated at 180 °C for 30 h. When the reaction was complete the autoclave was cooled to the room temperature. The products were washed with ethanol and deionized water several times and then separated by centrifugation. They were then dried at 60 °C for 1 h to obtain the precursors. Finally, the precursors were annealed at 300 °C for 2 h to produce the sample.

2.2 Characterization

The crystal structure of the sample was determined using X-ray diffraction (XRD, MAC Science, MXP18) and high-resolution transmission electron microscope (HRTEM, JEOL JEM-2010). The PL measurement was performed at the room temperature using the He–Cd laser line of 325 nm as an excitation source. The sample was mounted on a xyz-table which moved the sample to the intersection point of the laser beam and the optical axis to achieve better signal to noise ratio. The signals were collected with Olympus camera lens. Multiple curves were recorded to ensure the data reproducibility. The QY values were determined from the following equation:

$$\mathrm{QY(sample)} = \left(\mathrm{F_{sample}}/\ \mathrm{F_{ref}}\right)\left(\mathrm{A_{ref}}/\ \mathrm{A_{sample}}\right) \times \left(\mathrm{n^2_{sample}}/\ \mathrm{n^2_{ref}}\right)\mathrm{QY(ref)},$$

where F, A, and n are the measured fluorescence (area under the emission peak), absorbance at the excitation wavelength, and refractive index of the solvent respectively. PL spectra were spectrally corrected and quantum yields were determined relative to Rhodamine 6G (QY = 94 %) [32].

3 Results and discussion

The XRD patterns of the ZnSe QDs are shown in Fig. 1a. All the diffraction peaks can be well indexed as being in the hexagonal wurtzite phase, which is consistent with the

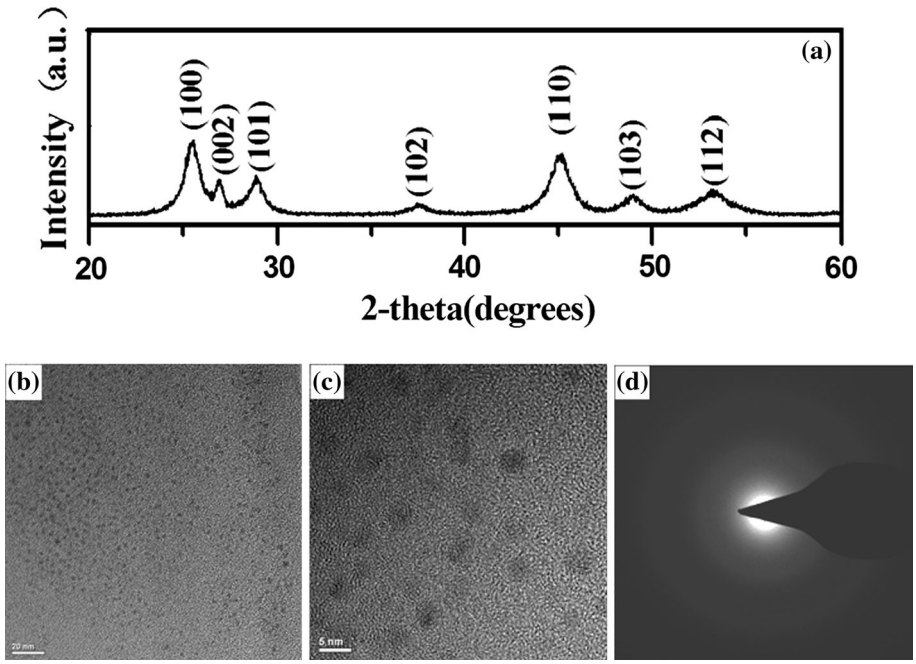

Fig. 1 XRD patterns (**a**), TEM image (**b**), HRTEM image (**c**) and the corresponding SAED pattern (**d**) of ZnSe QDs

standard card (P63mc, JCPDS No. 80-0008). No other diffraction peaks can be identified in the patterns, indicating no impurity exists in the sample. The diffraction peaks are broad and the intensities are low for the ZnSe QDs. In the diffraction patterns, peak broadening is mainly due to four factors: microstrains (deformations of the lattice), faulting (extended defects), crystalline domain size, and domain size distribution. Moreover, the lattice constant of 'a' and 'c' for the hexagonal structure can be determined from the following relations:

$$1/d_{hkl}^2 = 4/3\left\{\left(h^2 + hk + k^2\right)/a^2\right\} + \left(l^2/c^2\right)$$

The average lattice constants of 'a' and 'c' for the ZnSe QDs are found to be a = 3.999 Å, c = 6.568 Å and the corresponding c/a = 1.6426, which is slightly larger than the standard value of 1.6371. ZnSe are formed by coordinate covalent bonding. The lattice expansion can be correlated with the formation of vacancies in ZnSe QDs using the thermodynamic theory developed by Lu [33]. The free energy state of a finite size crystallite deviates from the ideal infinite crystal, and the deviation in free energy is found to be larger for smaller particles [34].

In order to clearly observe the particle size, TEM is used to characterize the sample. Figure 1b presents the TEM micrograph of the ZnSe QDs. These QDs are uniform and monodisperse, with an average diameter of about 4 nm. The wurtzite ZnSe QDs are also observed to be nearly spherical in shape, with a narrow size distribution. The HRTEM images and selected area electron diffraction (SAED) patterns of the ZnSe QDs are shown in Fig. 1c, d.

Based on the experiment results presented above, the growth mechanism for ZnSe QDs is proposed. When EN is added into the solution, Se powder is reduced by EN to Se^{2-}, which reacts with Zn^{2+} to form $ZnSe(EN)_{0.5}$, and this process is confirmed by the color change of the solution. The complexing reagent EN, which contains more than one N-chelating atom in each molecule, combines with Zn^{2+} and Se^{2-}, reducing the concentration of free Zn^{2+} and Se^{2-} greatly in the solution [35]. In the annealing treatment, EN is removed from the precursor, leaving ZnSe QDs once the synthesis is completed. The schematic illustration of this growth mechanism for ZnSe QDs is shown in Fig. 2. The possible growth mechanism can be described as follows:

$$Zn(NO_3)_2 \rightarrow Zn^{2+} + 2NO_3^- \quad (1)$$

$$Se + NH_2CH_2CH_2NH_2 \rightarrow Se^{2-} \quad (2)$$

$$Zn^{2+} + Se^{2-} + 0.5EN \rightarrow ZnSe \cdot EN_{0.5} \quad (3)$$

$$ZnSe \cdot EN_{0.5} \rightarrow ZnSe \downarrow + 0.5EN. \quad (4)$$

From the above explanation, it can be seen that EN acts not only as a strong alkali to activate Se to form Se^{2-} ions but also as a ligand to react with Zn^{2+} and Se^{2-} ions, forming $ZnSe(EN)_{0.5}$. The $ZnSe(EN)_{0.5}$ decomposes into ZnSe with a hexagonal structure after annealing. The formation and growth of the ZnSe QDs are slow processes because the second reaction is gradual. The complexing ability of groups containing N-chelating atom may affect the final synthesis phase due to the high coordination ability to zinc ($\log \beta[Zn(EN)_2]^{2+} = 10.83$) of EN [36].

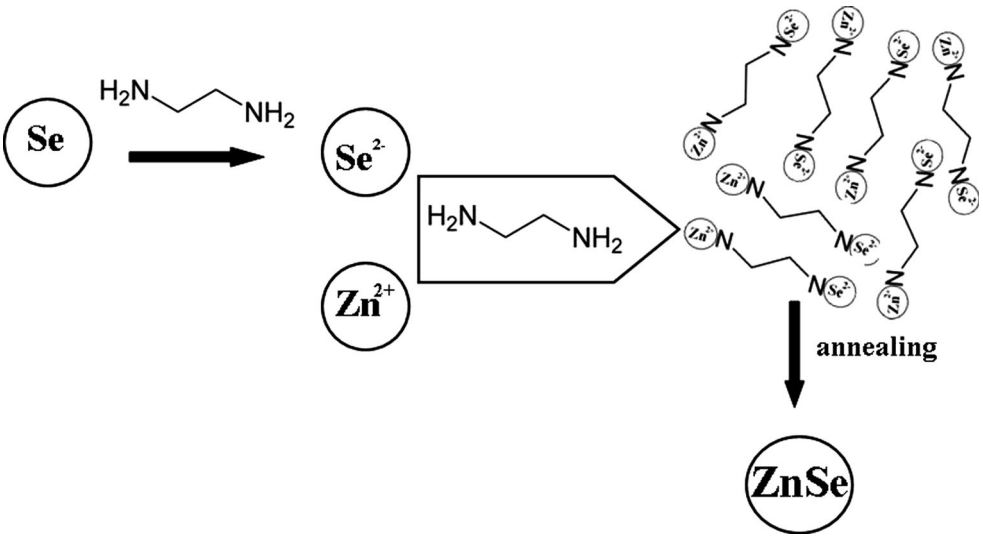

Fig. 2 Schematic illustrations of the growth mechanism for ZnSe QDs in which EN acts as a strong alkali and ligand

The optical performance of semiconductor materials is critically dependent on their constituent particle size. Figure 3 displays the room-temperature PL emission spectrum of the ZnSe QDs, which characterizes their optical properties. In Figure 3, the PL spectrum comprises two emission bands: a strong primary emission band centered at 422 nm, and a weak defect-related emission band extending from 500 to 640 nm. The primary emission band centered at 422 nm represents the near band-edge (NBE) emission of ZnSe [37]. It is blue-shifted relative to that for bulk ZnSe due to quantum confinement effects. An ultraviolet-blue (UV-blue) emission occurs above the band gap energy of bulk ZnSe (465 nm) and shifts to higher energies (422 nm) as the size of the ZnSe QD decreases (about 4 nm). Since the diameters of our ZnSe QDs are smaller than the Bohr radius of bulk ZnSe (4.5 nm), the Coulomb interaction should be small in our samples as the QDs are in the moderate to strong confinement regime [38]. In general, quantum confinement shifts the energy levels of the conduction and valence bands apart, giving rise to a blue shift in the transition energy as the particle size decreases [39]. The observation of such shifts suggests that this UV-blue luminescence results from the optical transitions between the discrete quantum-confined electron–hole states near the band edge for the ZnSe QDs. Theoretically, the energy of QDs can be written in simple form as: $E^{i}_{QD} = E_g + \frac{C_i}{R^{n_i}}$, where C_i and n_i are constants for certain materials. The size dependence of E_g for ZnSe is given by a power law expression, which can be written as: $E_g^{ZnSe}[d] = E_{g,\infty}^{ZnSe} + \frac{2.08}{d^{1.19}}$ [40, 41]. From this equation, the calculated average particlel size of the ZnSe QDs is 4.38 nm, which is close to what we measure. The PL spectrum of the ZnSe QDs (Fig. 3) shows a broad emission band between 500 and 640 nm, and this, we believe, can be attributed to Se

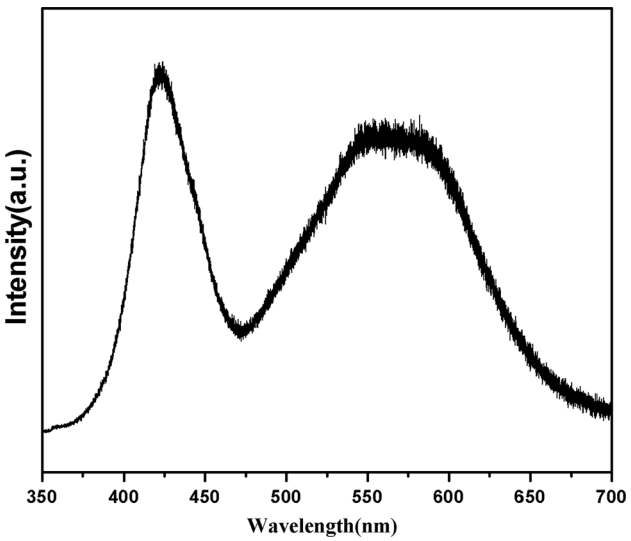

Fig. 3 Room-temperature PL spectrum of ZnSe QDs (excited at 325 nm)

vacancy, Zn vacancy and the presence of impurities [42–44]. Quantum yield of the as-prepared ZnSe QDs in aqueous solution is 5.4 %. Murase et al. [37, 45, 46] developed an alternative method to synthesize the blue emitting ZnSe nanocrystals in aqueous solution, and the product had low quantum yield (1–10 %). Our results are in agreement with the previous repots.

Figure 4 shows the room-temperature excitation-power dependent PL spectra of the ZnSe QDs. With the excitation power increasing, the NBE emission peak broadens. The intensity of the peak becomes stronger when the excitation power increases from 0.15 to 3 mW, and then decreases as the excitation power further increases to 30 mW. The NBE emission peak also displays an evident red shift with increasing excitation power. The inset in Fig. 4 shows that

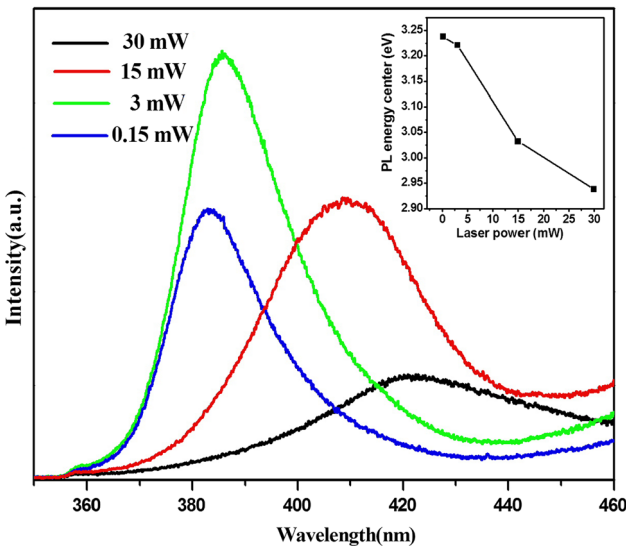

Fig. 4 Excitation-power-dependence of the PL spectra of ZnSe QDs, the*inset* pattern is the PL peak energy under different excitation power

the corresponding decrease in the peak energy can be as large as 300 meV.

Song et al. [47, 48] reported a red shift of the band-edge emission for the ZnO nanotetrapod and nanowire, which was due to the band-gap renormalization resulted from the screening of the Coulomb interaction, as well as exchange and correlation effects. Similar results were reported by Lyu et al. [49]. Red-shifting of the NBE emission peak with increasing excitation intensity may be explained from our experimental results as follows. In the electron–hole plasma (EHP) regime, the band gap is a monotonically decreasing function of increasing carrier density, due to the screening of the Coulomb interaction and exchange and correlation effects, which gives rise to the band gap renormalization with a red-shift of emissions [50]. When the carrier density increases, the excitonic state becomes destabilized and an EHP state is formed. In the EHP regime, the band gap usually decreases. Therefore, the emissions are red-shifted due to the band gap renormalization in the EHP regime with increasing excitation intensities [51].

4 Conclusion

In summary, we have successfully developed a safe, controllable, easy to use, solvothermal method for synthesizing ZnSe QDs with the hexagonal wurtzite structure. The average particle size was about 4 nm. The high coordination ability to zinc of EN played an important role in the formation of the ZnSe QDs. The room-temperature PL spectrum of the ZnSe QDs exhibited an NBE emission peak centered at 422 nm and a defect-related emission band extending from 500 to 600 nm, and we believed that this secondary peak could be attributed to Se vacancy, Zn vacancy and the presence of impurities. With increasing excitation power, the NBE emission peak of the ZnSe QDs was red-shifted towards the low-energy region and the corresponding peak energy decreased by up to 300 meV. Moreover, the intensity of the NBE emission peak at first increased, and then decreased with increasing excitation power. These results provide useful insights that may have wide applications in optoelectronic devices based on uniform-structured ZnSe nanocrystalline semiconductor materials.

Acknowledgments This work was financially supported by the National Programs for High Technology Research and Development of China (863) (Item No. 2013AA032202), the National Natural Science Foundation of China (Grant No. 61008051, 61178074, 11204104, 11254001, 61378085, 61308095).

References

1. J. Archana, M. Navaneethan, Y. Hayakawa, S. Ponnusamy, C. Muthamizhchelvan, Mater. Res. Bull. **47**, 1892 (2012)
2. P. Pericleous, M. Gazouli, A. Lyberopoulou, S. Rizos, N. Nikiteas, E.P. Efstathopoulos, Int. J. Cancer **131**, 519 (2012)
3. B. Dong, C. Li, G. Chen, Y. Zhang, Y. Zhang, M. Deng, Q. Wang, Chem. Mater. **25**, 2503 (2013)
4. S. Shen, Q. Wang, Chem. Mater. **25**, 1166 (2013)
5. L. Li, Z. Chen, Y. Hu, X. Wang, T. Zhang, W. Chen, Q. Wang, J. Am. Chem. Soc. **135**, 1213 (2013)
6. V.V. Nikesh, Amit D. Lad, A.D. Lad, S. Kimura, S. Nozaki, S. Mahamuni, J. Appl. Phys. **100**, 113520 (2006)
7. S. Shen, Y. Zhang, Y. Liu, L. Peng, X. Chen, Q. Wang, Chem. Mater. **24**, 2407 (2012)
8. S. Shen, Y. Zhang, L. Peng, Y. Du, Q. Wang, Angew. Chem. **123**, 7253 (2011)
9. S. Chang, Y. Dai, B. Kang, W. Han, D. Chen, Solid State Commun. **149**, 1180 (2009)
10. T.S. Kim, B.W. Lee, E. Oh, S. Lee, J.K. Furdyna, J. Appl. Phys. **107**, 063517 (2010)
11. L. Zhang, X. Shen, H. Liang, J. Yao, J. Phys. Chem. C **114**, 21921 (2010)
12. J. Jung, K. Zhou, J. Bang, J. Lee, J. Phys. Chem. C **116**, 12409 (2012)
13. J. Archana, M. Navaneethan, Y. Hayakawa, S. Ponnusamy, C. Muthamizhchelvan, Mater. Res. Bull. **47**, 1892 (2012)
14. M. Sharma, S.K. Tripathi, J. Phys. Chem. Solids **73**, 1075 (2012)
15. A.B. Panda, S. Acharya, S. Efrima, Y. Golan, Langmuir **23**, 765 (2007)
16. P. Reiss, New J. Chem. **31**, 1843 (2007)
17. Y.M. Sung, K.S. Park, Y.J. Lee, J. Phys. Chem. C **111**, 1239 (2007)
18. J. Bang, J. Park, J.H. Lee, N. Won, J. Nam, J. Lim, B.Y. Chang, H.J. Lee, B. Chon, J. Shin, J.B. Park, J.H. Choi, K. Cho, S.M. Park, T. Joo, S. Kim, Chem. Mater. **22**, 233 (2010)
19. A. Antonello, M. Guglielmi, V. Bello, G. Mattei, A. Chiasera, M. Ferrari, A. Martucci, J. Phys. Chem. C **114**, 18423 (2010)
20. X. Di, S.K. Kansal, W. Deng, Sep. Purif. Technol. **68**, 61 (2009)

21. S.A. Santangelo, E.A. Hinds, V.A. Vlaskin, P.I. Archer, D.R. Gamelin, J. Am. Chem. Soc. **129**, 3973 (2007)
22. J.J. Andrade, A.G. Brasil Jr, P.M.A. Farias, A. Fontes, B.S. Santos, Microelectron. J. **40**, 641 (2009)
23. F.Y. Shen, W. Que, X.T. Yin, Y.W. Huang, Q.Y. Jia, J. Alloys Compd. **509**, 9105 (2011)
24. S. Mahamuni, A.D. Lad, S. Patole, J. Phys. Chem. C **112**, 2271 (2008)
25. M.A. Hines, P. Guyot-Sionnest, J. Phys. Chem. B **102**, 3655 (1998)
26. X. Wang, J. Zhu, Y. Zhang, J. Jiang, S. Wei, Appl. Phys. A **99**, 651 (2010)
27. M.G. Syed Basheer Ahamed, V.S. Nagarethinam, A.R. Balu, A. Thayumanavan, K.R. Murali, C. Sanjeeviraja, M. Jayachandran, Cryst. Res. Technol. **45**, 421 (2010)
28. B. Geng, J. You, F. Zhan, M. Kong, C. Fang, J. Phys. Chem. C **112**, 11301 (2008)
29. H.W. Zhu, P.G. Li, M. Lei, L.H. Li, S.L. Wang, W.H. Tang, J. Alloys Compd. **509**, 3306 (2011)
30. L. Zhang, H. Yang, Appl. Phys. A **98**, 801 (2010)
31. D. Albert, J. Nurnberger, V. Hock, M. Ehinger, W. Faschinger, G. Landwehr, Appl. Phys. Lett. **74**, 1957 (1999)
32. M. Fischer, J. Georges, Chem. Phys. Lett. **260**, 115–118 (1996)
33. K. Lu, M.L. Sui, J. Mater. Sci. Tech. **9**, 419 (1993)
34. A. Aboulaich, M. Geszke, L. Balan, J. Ghanbaja, G. Medjahdi, R. Schneider, Inorg. Chem. **49**, 10940 (2010)
35. T.S. Li, S.P. Liu, Z.X. Lu, Z.F. Liu, Chin. Chem. Lett. **18**, 617 (2007)
36. J.H. Zhan, X.G. Yang, W.X. Zhang, D.W. Wang, Y. Xie, Y.T. Qian, J. Mater. Res. **15**, 629 (2000)
37. H.S. Chen, B. Lo, J.Y. Hwang, G.Y. Chang, C.M. Chen, S.J. Tasi, S.J.J. Wang, J. Phys. Chem. B **108**, 17119 (2004)
38. B. Pejova, J. Solid State Chem. **181**, 1961 (2008)
39. N. Revaprasadu, M.A. Malik, P. O'Brien, M.M. Zulu, G. Wakefield, J. Mater. Chem. **8**, 1885 (1998)
40. C.A. Smith, H.W.H. Lee, V.J. Leppert, S.H. Risbud, Appl. Phys. Lett. **75**, 1688 (1999)
41. S.A. Santangelo, E.A. Hinds, V.A. Vlaskin, P.I. Archer, D.R. Gamelin, J. Am. Chem. Soc. **129**, 3973 (2007)
42. J. Li, M. Wang, X. Wang, X. Huo, Yao, Ceram. Int. **34**, 1077 (2008)
43. B. Xi, S. Xiong, D. Xu, J. Li, H. Zhou, J. Pan, J. Li, Y. Qian, Chem. Eur. J. **14**, 9786 (2008)
44. H. Wang, T. Tian, S. Yan, N. Huang, Z. Xiao, J. Cryst. Growth **311**, 3787 (2009)
45. N. Murase, M.Y. Gao, Mater. Lett. **58**, 3898 (2004)
46. N. Murase, M.Y. Gao, N. Gaponik, T. Yazawa, J. Feldmann, Int. J. Modern Phys. B **15**, 3881 (2001)
47. J.K. Song, J.M. Szarko, S.R. Leone, S. Li, Y. Zhao, J. Phys. Chem. B **109**, 15749 (2005)
48. J.K. Song, U. Willer, J.M. Szarko, S.R. Leone, S. Li, Y. Zhao, J. Phys. Chem. C **112**, 1679 (2008)
49. S.C. Lyu, Y. Zhang, H. Ruh, H. Lee, H. Shim, E. Suh, C.J. Lee, Chem. Phys. Lett. **363**, 134 (2002)
50. F.P. Logue, P. Rees, J.F. Heffernan, C. Jordan, J.F. Donegan, J. Hegarty, Phys. Rev. B **54**, 16417 (1996)
51. J. Takeda, H. Jinnouchi, S. Kurita, Y.F. Chen, T. Yao, Phys. Stat. Sol. b **229**, 877 (2002)